Hot-Film and Hot-Wire Anemometry for a Boundary Layer Active Flow Control Test

K. Lenahan[1]
School of Electrical Engineering
Stanford University, Stanford, CA 94309

D. Schatzman[2]
Science and Technology Corporation, Ames Research Center
Moffett Field, CA 94035

and

J. Wilson[3]
Aviation Development Directorate - AFDD
U.S. Army Research, Development, and Engineering Command (AMRDEC)
Moffett Field, CA 94035

Unsteady active flow control (AFC) has been used experimentally for many years to minimize "bluff-body" drag. This technology could significantly improve performance of rotorcraft by cleaning up flow separation. It is important, then, that new actuator technologies be studied for application to future vehicles. A boundary layer wind tunnel was constructed with a 1ft-x-3ft test section and unsteady measurement instrumentation to study how AFC manipulates the boundary layer to overcome adverse pressure gradients and flow separation. This unsteady flow control research requires unsteady measurement methods. In order to measure the boundary layer characteristics, both hot-wire and hot-film Constant Temperature Anemometry is used. A hot-wire probe is mounted in the flow to measure velocity while a hot-film array lays on the test surface to measure skin friction. Hot-film sensors are connected to an anemometer, a Wheatstone bridge circuit with an output that corresponds to the dynamic flow response. From this output, the time varying flow field, turbulence, and flow reversal can be characterized. Tuning the anemometers requires a fan test on the hot-film sensors to adjust each output. This is a delicate process as several variables drastically affect the data, including control resistance, signal input, trim, and gain settings.

Nomenclature

b	=	spanwise length scale of SaOB actuator; 1.66 in.
BR	=	bridge ratio; $R_C / R_H = 5$
OH	=	overheat ratio; $R_H / R_S = 1.5$
R_H	=	operating resistance of hot-film sensor at t_h
R_0	=	ice point resistance of hot-film sensor at t_0
R_S	=	resistance of hot-film sensor at ambient fluid temperature
R_C	=	resistance of control resistor; $(R_S)*(BR)*(OH)$

---

[1] Undergraduate Student, School of Electrical Engineering, Stanford University.
[2] Research Engineer, Aviation Development Directorate – AFDD, Ames Research Center/M.S. 215-1.
[3] Research Engineer, Aviation Development Directorate – AFDD, Ames Research Center/M.S. 215-1.

t_0 =   ice point temperature of hot-film sensor or temperature coefficient of sensor resistance at 0°C

t_h =   operating temperature of hot-film sensor

x =   streamwise coordinate

z =   spanwise coordinate

I. Introduction

Active Flow Control (AFC) using steady suction and oscillatory blowing (SaOB) and synthetic jet actuators remains an important area of research today. If these kinds of actuators can be improved and implemented into future flight vehicles, they could enhance rotorcraft performance. SaOB actuators have already proven to significantly reduce drag when tested on an axisymmetric model in results by Wilson et al.[1] and Schatzman et al.[2] These studies were motivated by Arwatz et al.[3] and the development of a SaOB actuator with no moving parts that achieved near-sonic output at high efficiency. This test uses five SaOB actuators next to each other in a spanwise array.

Synthetic jet actuators and their interactions with the turbulent boundary layer have also been studied by Schaeffler et al.[4] and Ramasamy et al.[5] Schaeffler et al. studied synthetic jets using laser-Doppler velocimetry (LDV), 2-D particle image velocimetry (PIV) and stereo PIV to help validate AFC databases. Ramasamy et al. used μ-PIV, which has a reduced viewing area (~40-μm) to better understand the synthetic jet's high-velocity gradient flow field and associated small-scale rotational coherent structures. Unlike the SaOB actuators, synthetic jets are electrically driven by a sinusoidal signal from a power amplifier to create suction and blowing through an angled opening along the test surface. This test uses six synthetic jets spaced uniformly across a 30 inch spanwise slot.

This study utilized time-averaged and phase-averaged hot-wire measurements as well as hot-film anemometry, which was primarily for analyzing skin friction. This yields measurements of the time-varying flow field, turbulence, and flow reversals. Zhang et al.[6] showed that hot-film measurements were more accurate than surface static pressure measurements when studying boundary layer separation and reattachment from the mean quasi-wall-shear stress. These studies also were able to identify the transition state of the attached and separated sheer layer. The primary purpose of this study is to see how SaOB and synthetic jet actuators interact with a zero pressure gradient (ZPG) turbulent boundary layer and influence the reattachment of separated flows in an adverse pressure gradient (APG). Therefore, hot-film measurements were essential to this unsteady boundary layer test. The experimental facility, as shown in Fig. 1, consists of a boundary layer wind tunnel with a 1ft-x-3ft test section, with multiple actuator inserts, and a pliable roof to adjust pressure gradients.
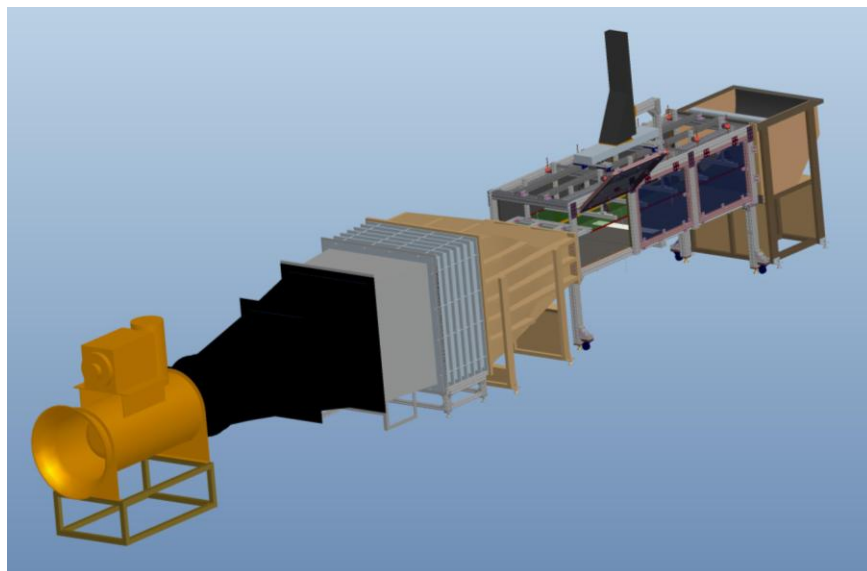

Figure 1. The Boundary Layer Tunnel (BLT) that will be used to test both synthetic jet and SaOB actuators using hot-wire and hot-film anemometry.

II. Setup for Experiment

In order to prepare for this experiment, ten TSI 1750 anemometers needed to be selected, tested, and reconnected to the test bed rack, see Fig. 2. Thirty of these existed from a previous study[7] at NASA Ames however, some were no longer functional. On the left is the external cover of the anemometer and on the right is the internal circuit. The hot-film sensor is connected at the inputs A and B, the control resistor at inputs C and D, the output signal at E and F, and the power and ground at inputs G and H, respectively. The trim inductor can be seen in the upper right hand of the circuit, as well as the gain wiper just below it. These anemometers were set up in sets of three per board in the test rack and shared power and ground accordingly.

The basic design of each 1750 anemometer is a Wheatstone bridge with the hot-film sensor connected into the bridge circuitry. Figure 3 shows the 1750 TSI Constant Temperature Anemometer circuit diagram. The arrows on the trim, gain control, and control resistor represent variable wipers. It can be seen here that the hot-film sensor is part of the Wheatstone bridge, which keeps the hot-film sensor at a constant temperature and results in an output signal based on the voltage supplied to the sensor. The hot-film sensor and the control resistor represent two legs of the Wheatstone bridge in which the hot-film sensor is the probe and the control resistor sets the operating temperature of the probe.
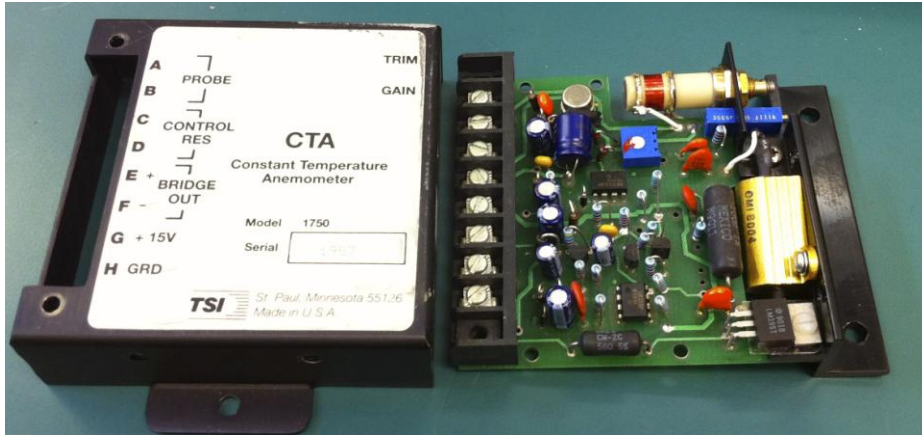

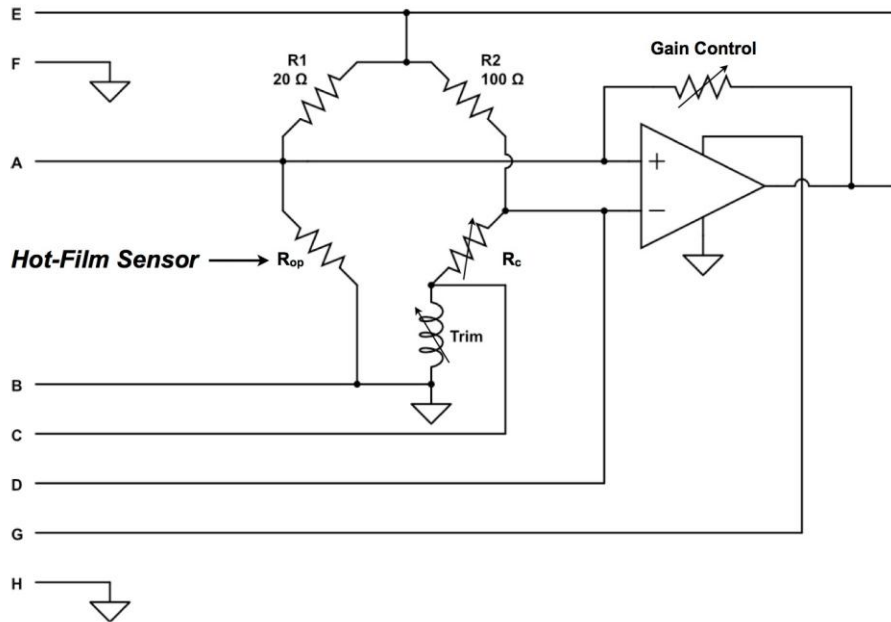**Figure 2. 1750 TSI Constant Temperature Anemometer.**

Figure 3. 1750 TSI Constant Temperature Anemometer circuit diagram.

In order to test these anemometers, each was removed from the original test rack, connected to a bench top voltage source, hot film sensor, control resistor, and Agilent Technologies DSO7014B 100 MHz, four-channel oscilloscope. A small fan was then used to blow a test flow over the hot-film sensor. The first adjustment that was necessary was to bring each anemometer out of the "ringing" range, which appeared as a distorted resonant sine wave on the oscilloscope, or an unstable feedback. By adjusting the trim, an inductor control in the anemometer, the anemometer's output could be brought back into the readable range, which shows the turbulence flowing over the hot-film sensor. The gain control was irrelevant in this stage of anemometer testing because it only becomes effective at flow speeds much greater than the test fan. The control resistor, however, was important in properly preparing the anemometers for a bench top test.

The primary purpose of the control resistor is to set the overheat temperature of the hot-film sensor. By observing the varying amount of voltage transmitted to the film to maintain a constant temperature, the dynamic skin friction can be qualitatively observed. In the previous study, the anemometers' overheat ratio was set to 1.5. Overheat ratio, OH, is governed by this equation:

$$OH = R_H / R_S \tag{1}$$

where R_H is the operating resistance of the hot-film sensor and R_S is the resistance of hot-film sensor at ambient fluid temperature. R_S can be easily determined with an ohmmeter and the hot-film sensor at ambient temperature. Operating resistance can then be found via this equation:

$$R_H = R_0[1 + .(t_h - t_0)] \tag{2}$$

where R_0 is the ice point resistance of the sensor at t_0, the ice point temperature, and t_h is operating temperature of the hot-film sensor. The control resistance, R_C, can then be found using the following equation:

$$R_C = (R_S) * (BR) * (OH) \tag{3}$$

Here the bridge resistance $BR = 5$ for the 1750 TSI anemometers. Once the overheat ratio is set and the trim is adjusted out of "ringing", a signal can be seen on the oscilloscope for the flow. At this point, if the signal is clear, the anemometer is ready for a bench top test with the actuators. This equation can also be rearranged to easily solve for R_H when R_C is already known.

Figure 4 shows the hot-film sensors used for initial checkouts. Each sensor in this hot-film array averages approximately 11.2 ohms of resistivity. New hot-film arrays will be used in future experimentation in the new BLT tunnel. Figure 5 shows a schematic of the Senflex 93112 hot-film array that will be mounted on the floor of the BLT tunnel upon completion downstream of the slots for each type of actuator. These sensors will have a resistivity of about 6-8 ohms, using a lead resistance of <0.05 ohms/in.

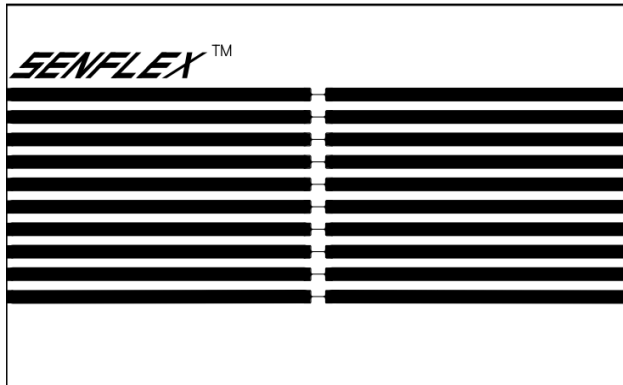**Figure 4. Hot-film array used in checkout of the anemometers used in this study.**

Figure 5. Senflex 93112 hot-film array schematic.

III. Results

The results from the benchtop test setup will be used to help aid design decisions for the final hot-film setup in the BLT upon its first test. In the benchtop test setup, a plate with the hot-film sensors used to calibrate the 1750 anemometers was attached flush next to two SaOB actuators. Figure 6 shows this setup and the tick marks designating where the hot-film plate was shifted to measure the actuators' flow. The coordinate system was defined such that z represents the spanwise measurement while x represents the streamwise direction, and the origin is centered between the two actuators and located at the downstream edge of the pulse blowing slots. These coordinates were non-dimensionalized by a length scale equal to the spanwise spacing between the two actuator centerlines, $b = 1.66$ in. Four hot-film signals were measured at a sample rate of 10 kHz for 5 seconds, with the array centered at spanwise locations of $z/b = 0.00$, $z/b = 0.25$, and $z/b = 0.50$. The sensors were located downstream of the pulse blowing slots at streamwise locations of $x/b = 1.13$, 1.34, 1.37, and 1.39.

Compressed air was run through the actuators to observe the dynamic response of the hot-film sensors and checkout the data acquisition system. Figure 7 shows instantaneous hot-film signals for the three different spanwise measurement locations. Figure 7(a) shows that the blowing from both actuators mixes across the hot-film sensors. When the plate is slid to the right in Fig. 7(b), the sensors start to only pick up the flow from the left nozzle of actuator #2, and upon reaching z/b = .5 in Fig. 7(c), hardly any flow is experienced by the hot-film sensors at all, as the sensor array is centered on the splitter plate of the pulse blowing slots. Even from this raw data, periodicity can be observed in all three plots.
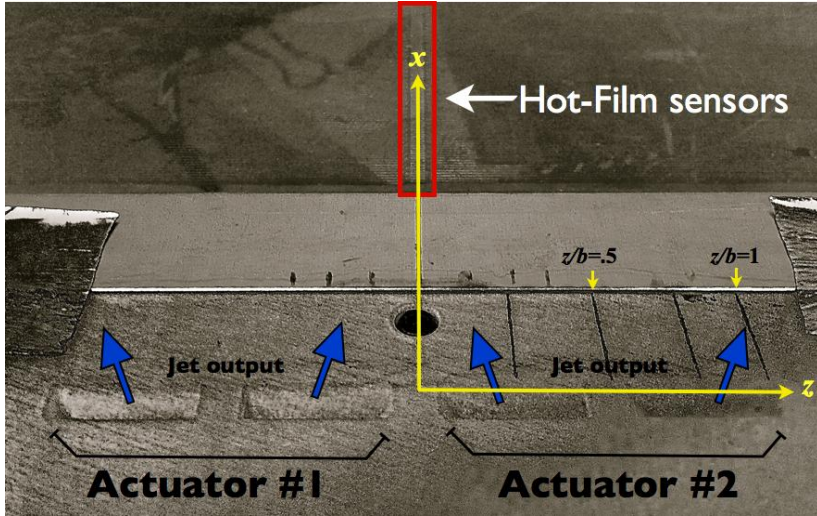
Figure 6. SaOB actuator benchtop setup with hot-film sensor array flush mounted downstream of oscillatory blowing surface slots.
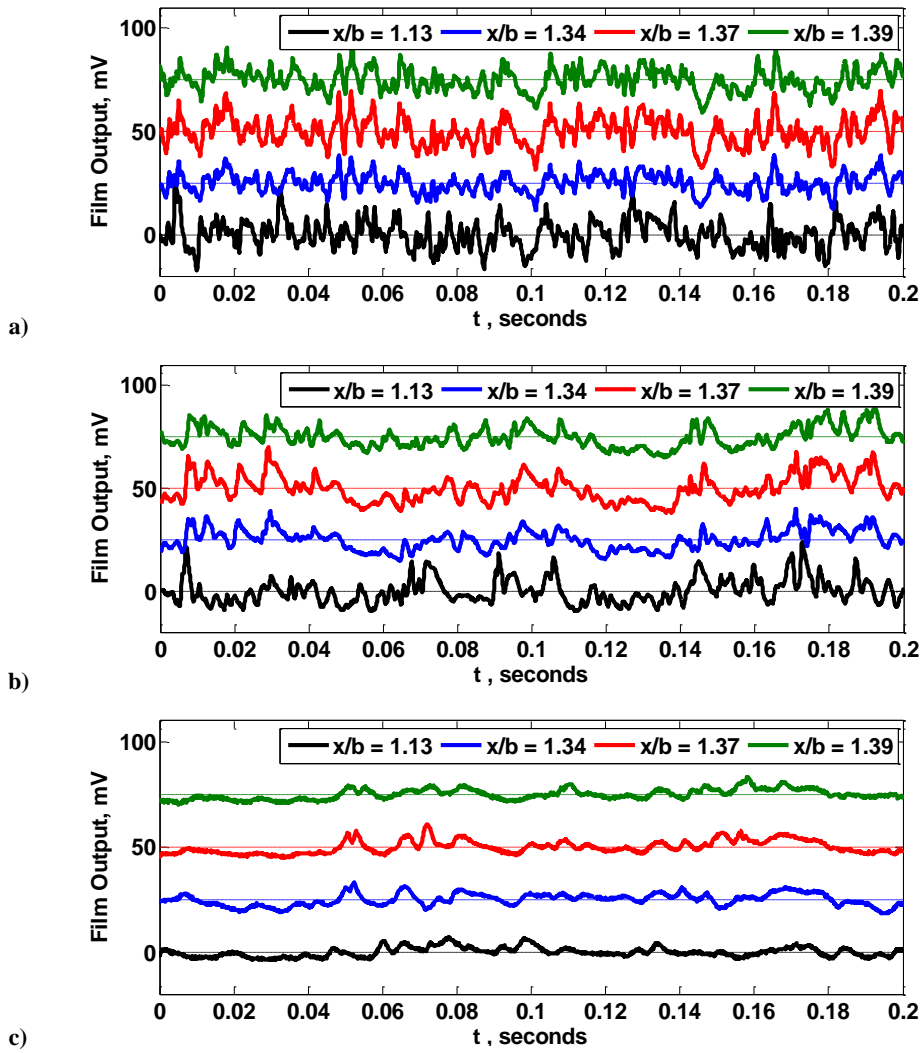

Figure 7. Four instantaneous hot-film a.c. signals measured downstream of the oscillatory blowing surface slots at a) z/b = 0.00 b) z/b = 0.25 and c) z/b = 0.50. (Arbitrary D.C. voltage offset added for plotting clarity)

A signal from a 1 psid Kulite differential pressure transducer, connected across the feedback tube of actuator #2, was used as phase reference for the instantaneous hot-film signals. The 5 second time series for each hot-film signal was phase locked with the pressure signal, which had an average oscillation frequency of 162 Hz. The phase average results for the three spanwise measurement locations are shown in Fig. 8. Note that for Figures 8(a) and 8(b), the phase response of the measurements at the upstream location of x/b = 1.13 have a phase shift with respect to the three signals measured farther downstream at x/b = 1.34, 1.37 and 1.39. Figure 8(c) shows that the spanwise location at z/b = 0.50, downstream of the pulsed blowing slots splitter plate, does not show any phase response.
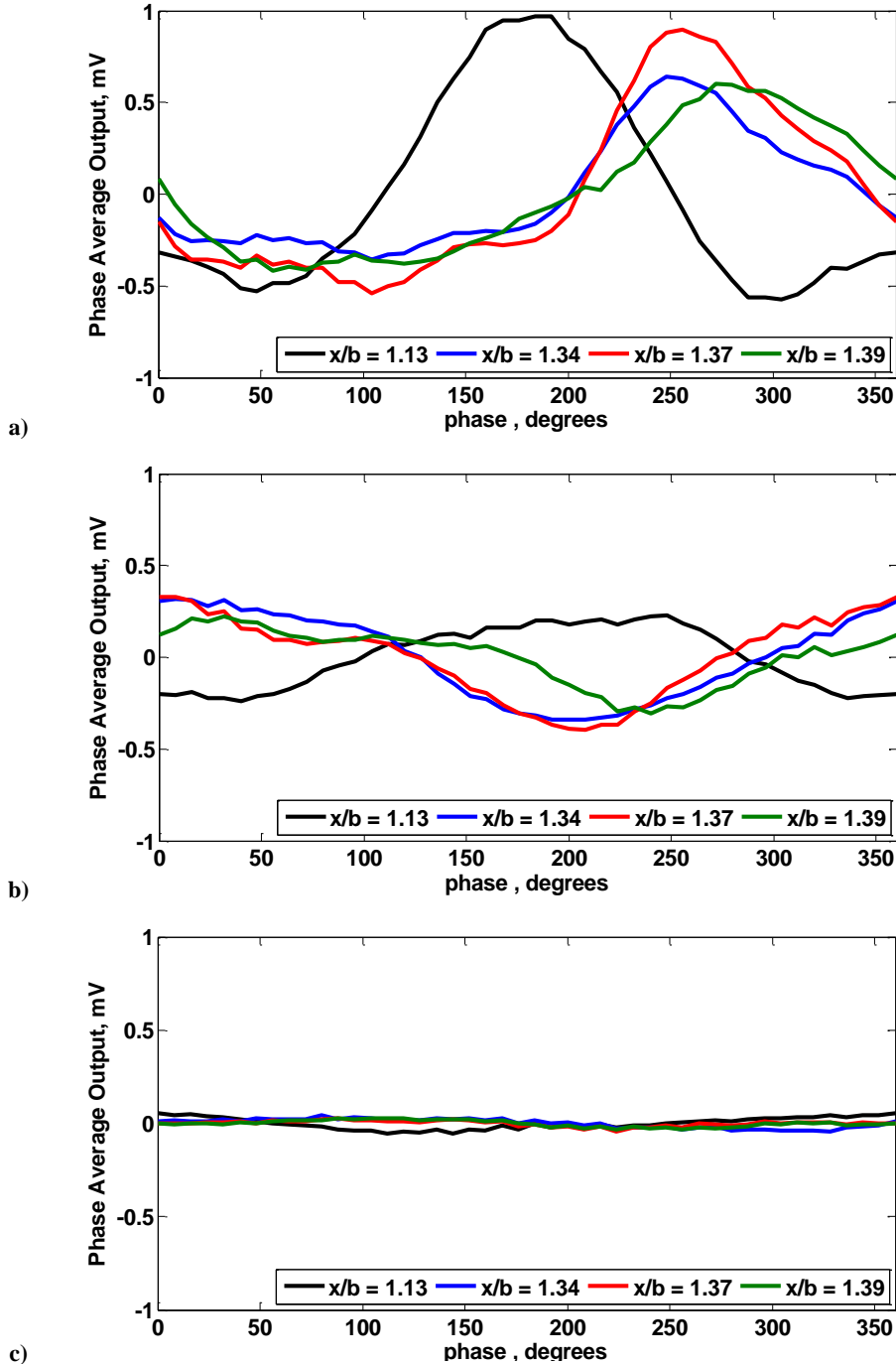

Figure 8. Phase-averaged hot-film signals measured downstream of the oscillatory blowing surface slots at a) z/b = 0.00 b) z/b = 0.25 and c) z/b = 0.50.

IV. Conclusion

In this study a ten-anemometer system was set up, tested and calibrated with hot-film sensors in a boundary layer wind tunnel. After the system was set up and properly working, it was applied to a bench test mockup of the wind tunnel hardware. When the hot-film anemometry system was tested with two SaOB actuators, results show that the raw data has periodicity. The hot-film output was phase-locked with the pressure measured across the SaOB actuator feedback tube. Flow field, turbulence, and flow reversals will be more apparent after time and phase-averaging the data. This hot-wire system will be used in the BLT for future tests with synthetic jet and SaOB actuators to gain understanding of unsteady flow.

References

[1] Wilson, J., Schatzman, D., Arad, E., Seifert, A., Shtendel, T., "Suction and Pulsed-Blowing Flow Control Applied to an Axisymmetric Body".

[2] Schatzman, D., Wilson, J., Arad, E., Seifert, A., Shtendel, T., "Flow Physics of Drag Reduction Mechanism using Suction and Pulsed Blowing" AIAA Aerospace Sciences Meeting, 07-10, January 2013.

[3] Arwatz, G., Fono, I., Seifert, A., "Suction and Oscillatory Blowing Actuator Modeling and Validation" AIAA Journal, Vol. 46, No. 5, May 2008.

[4] Schaeffler, N., Jenkins, L., "Isolated Synthetic Jet in Crossflow: Experimental Protocols for a Validation Dataset" AIAA Journal, Vol. 44, No. 12, December 2006.

[5] Ramasamy, M., Wilson, J., Martin, P., "Interaction of Synthetic Jet with Boundary Layer Using Microscopic Particle Image Velocimetry" AIAA Journal of Aircraft, Vol. 47, No. 2, March-April 2010.

[6] Zhang, X.F., Mahallati, A., Sjolander, S.A., "Hot-Film Measurements of Boundary Layer Transition, Separation and Reattachment on a Low-Pressure Turbine Airfoil at Low Reynolds Numbers" AIAA Joint Propulsion Conference, 7-10, July 2002.

[7] Chandrasekhara, M.S., Wilder, M.C., "Heat-Flux Gauge Studies of Compressible Dynamic Stall" AIAA Journal, Vol. 41, No. 5, May 2003.